Title: Opto-Acoustic Breast Imaging – Imaging-Pathology Correlation of Opto-Acoustic Features Respecting Malignancy

Authors: R S Butler, MD; A T Stavros, MD; P T Lavin, PhD; M J Ulissey, MD; F L Tucker, MD

Purpose

Opto-acoustic (OA) Imagio® (Seno Medical Instruments, San Antonio, TX) is a novel investigational device (Figure 1) with functional modality that integrates laser optics with ultrasound in an effort to improve the performance of currently available breast imaging modalities without the use of IV contrast or ionizing radiation. A fusion of anatomic and functional modalities, OA imaging provides both conventional B-mode images and co-registered real time color maps that demonstrate tumor vascularity and the relative amount of hemoglobin oxygenation within and around breast tumors. The technology is based on the observation that malignant tumors must generate neovessels to grow larger than 2 mm and are also more metabolically active, extracting oxygen from hemoglobin to a greater degree than benign neoplasms or normal tissue [1, 2]. This added information may help differentiate benign from malignant masses even when their gray-scale sonographic morphologic features overlap.

Figure 1. The Imagio™ device integrates laser light optics with conventional B-mode ultrasound to provide both anatomic and functional information.
References: Seno Medical Instruments, San Antonio, TX/US

In contrast to conventional ultrasound, which both emits and receives high-frequency sound waves, OA imaging emits short pulses of laser light at two wavelengths that correspond to the absorption peaks of oxygenated (1064 nm) and deoxygenated (757 nm) hemoglobin. These very brief bursts of low energy laser cause a momentary heating and expansion of blood, which is detected and color-coded as green for oxygenated hemoglobin and red for deoxygenated hemoglobin. The color-coded, opto-acoustic data is co-registered with the gray-scale ultrasound image in real time (Figure 2). In this study, we correlated OA imaging findings with

histopathologic features of breast cancers to elucidate the histopathologic basis for the findings of this new functional imaging platform.

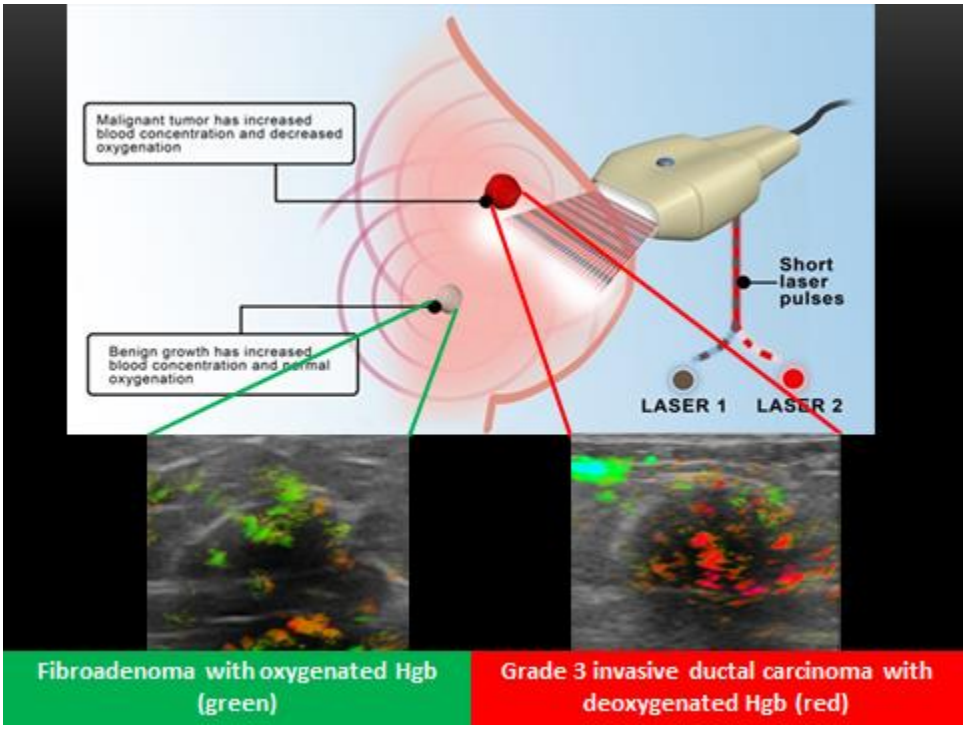

Figure 2. Laser light emitted at wavelengths corresponding to the absorption peaks of oxygenated and deoxygenated hemoglobin produces color-coded maps reflecting the level of oxygenation within benign and malignant tumors.
References: Seno Medical Instruments, San Antonio, TX/US

Methods and Materials

Study Design

After initial clinical validation, a Health Insurance Portability and Accountability Act (HIPAA)-compliant institutional review board (IRB)-approved Feasibility Study of OA imaging was undertaken. 155 patients with solid breast masses assessed as BI-RADS 3, BI-RADS 4, or BI-RADS 5 on conventional diagnostic ultrasound imaging were enrolled with informed consent. All of these patients were subsequently scanned with OA imaging at one of two IRB-approved

sites. 79 lesions were biopsied yielding 39 benign and 34 malignant results, with 6 lesions excluded, for a final study population of 30 malignancies. All tumors were evaluated with OA prior to biopsy and underwent standardized histopathology after biopsy.

Imaging Assessment

A scanning protocol was established, which consisted of both conventional B-mode and OA images. Prior to initializing the laser, gray-scale images in the radial and anti-radial planes were obtained with and without measurements in three planes. Subsequently, the laser was activated and the images were repeated. The OA images were viewed as a 6:1 display of the conventional gray-scale image together with five different OA maps consisting of gray long and short wave images and 3 color maps (Figure 3). OA features based on pre-biopsy imaging were analyzed by a radiologist with >30 years of expertise in breast ultrasound (ATS) who was blinded to the histopathology. OA imaging revealed three distinct zones within breast malignancies – tumor interior, boundary zone, and periphery. Using predefined measures, an OA score was calculated for each zone based on the relative amount of detected hemoglobin (hemoglobin score), the number of individually resolved vessels (vessel score) and the degree of tumor blush representing vessels too small to resolve (blush score). The total OA score was calculated as a sum of the above. The internal OA score was based on features within the tumor interior, while the external OA score combined the features of the tumor boundary zone and periphery.

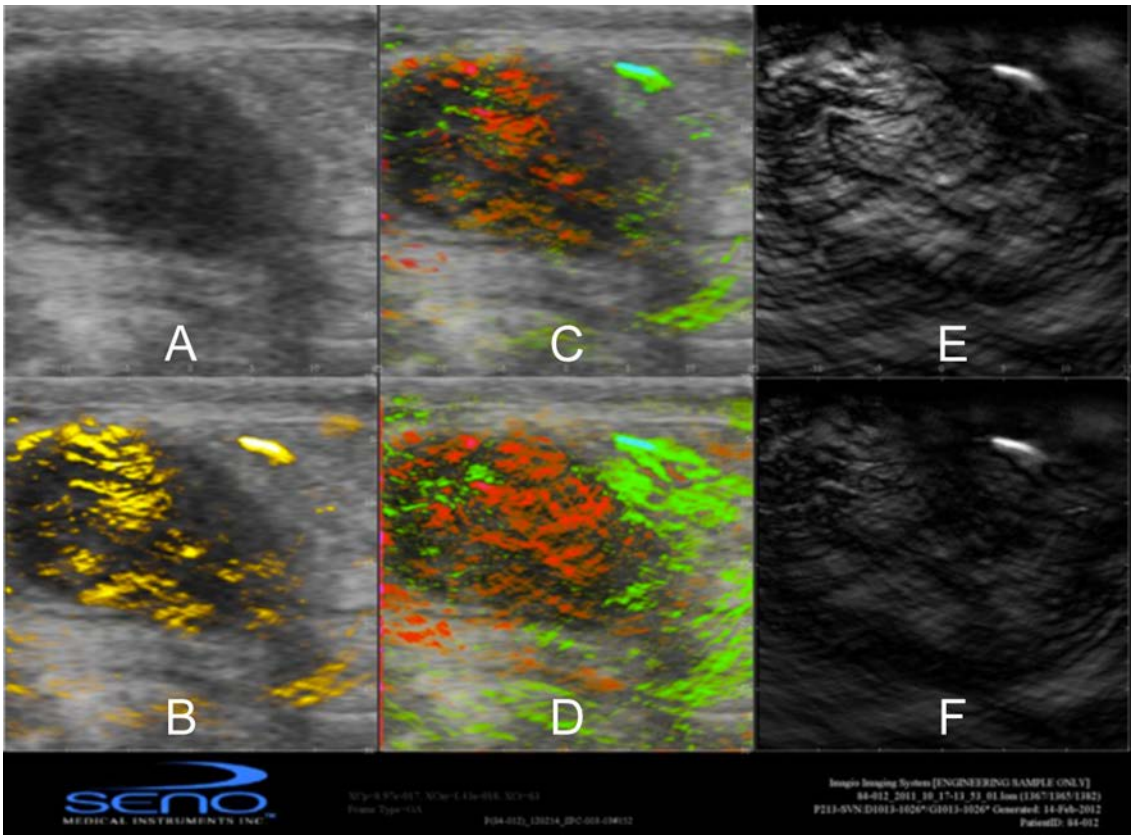

Figure 3. The Imagio 6:1 display: A. B-mode conventional ultrasound image shows oval mass with partially circumscribed and partially indistinct margins. B. Total map showing the regions of greatest blood flow within the image indicates increased vascularity within the tumor interior. C. Combined map showing the level of oxygenation within the regions of greatest blood flow reveals the hemoglobin within the tumor vessels to be deoxygenated, color coded as red. D. Relative map shows the relative degree of oxygenation within the imaged region. Information contained in the relative map is synthesized from the gray scale OA short wavelength (E) and and gray scale OA long wavelength (F) maps.
References: Seno Medical Instruments, San Antonio, TX/US

Histopathologic Evaluation

The tissue cores were evaluated by an independent pathologist with >30 years of experience in breast pathology (FLT) who was blinded to the OA imaging features. Histologic assessment was based on standard hematoxylin and eosin (H&E) stains. Measures of histologic grade based on

Scarff-Bloom-Richardson (SBR) score, including tubule formation (SBR-T), nuclear atypia (SBR-N), and mitotic count (SBR-M), as well as total score (SBR-TOTAL) were recorded.

Statistical Analysis

Total internal and external OA scores were compared with histopathology measures using ANOVA and Spearman's rank correlation coefficients. The significance level was 0.05.

Results

The total internal OA score, calculated as the sum of the hemoglobin score, vessel score, and blush score within the tumor interior, correlated positively with histopathologic measures of tumor grade, though the correlations did not achieve statistical significance (Figure 4).

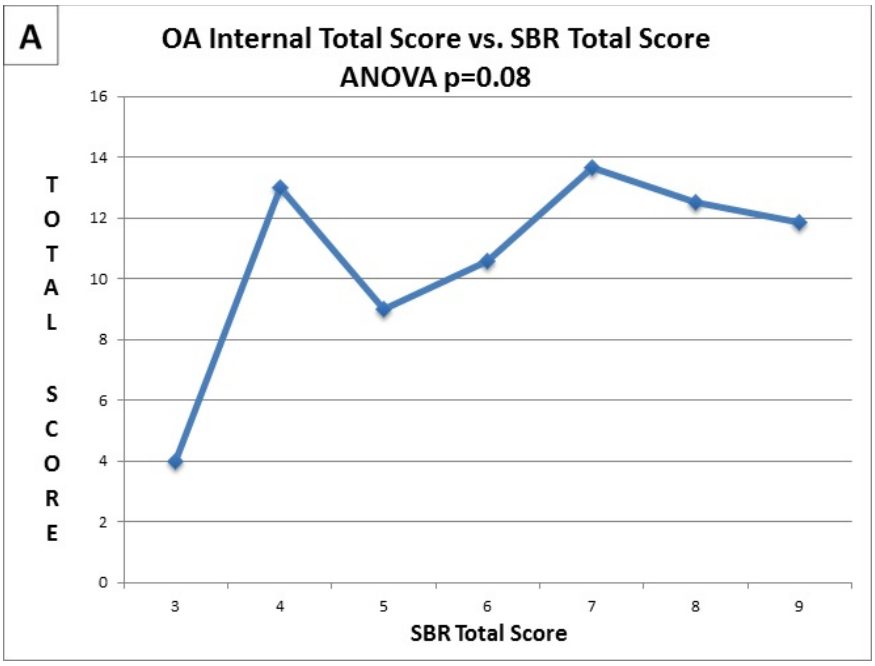

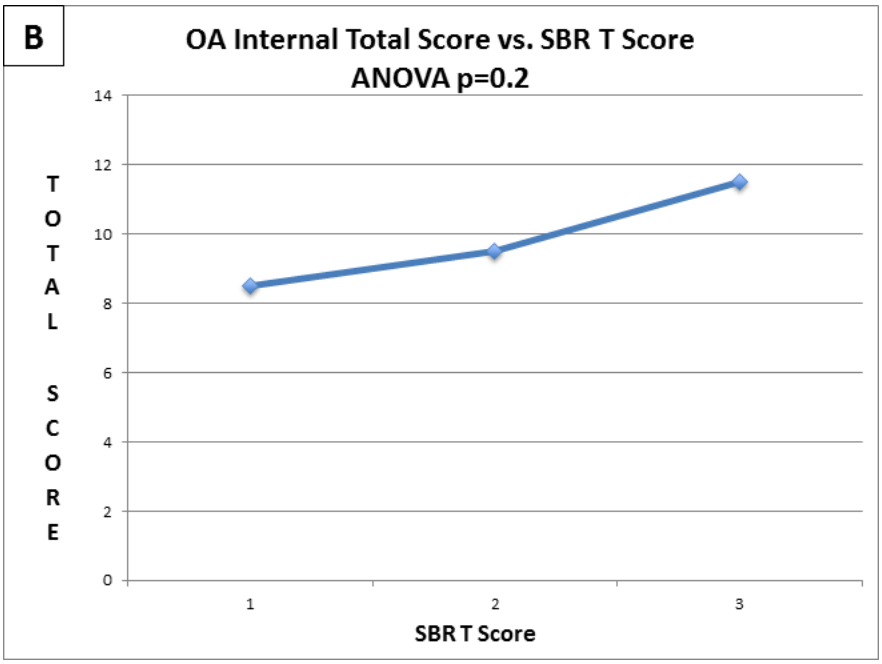
B
OA Internal Total Score vs. SBR T Score
ANOVA p=0.2
TOTAL SCORE
0
2
4
6
8
10
12
14
1
2
3
SBR T Score

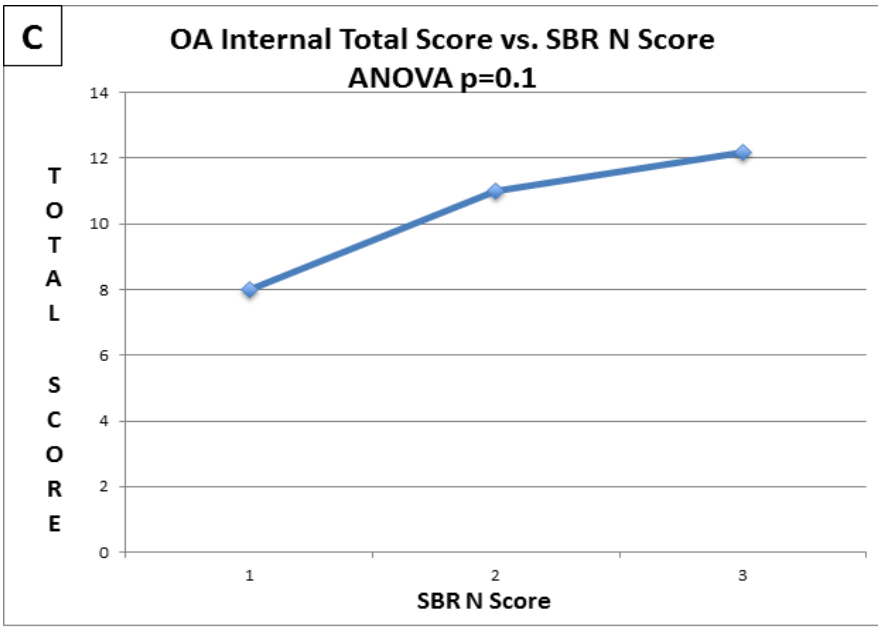
C
OA Internal Total Score vs. SBR N Score
ANOVA p=0.1
TOTAL SCORE
0
2
4
6
8
10
12
14
1
2
3
SBR N Score

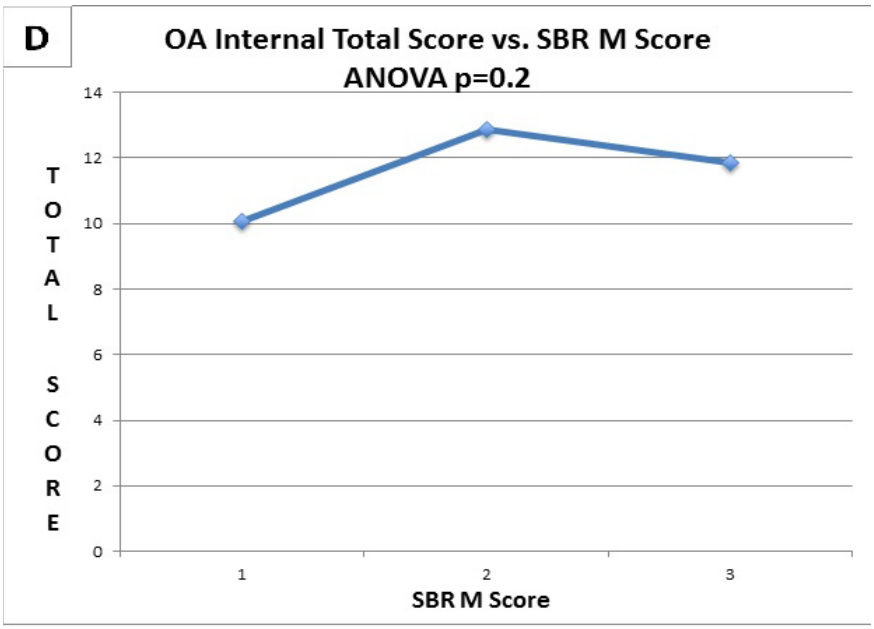

Figure 4. Correlation of internal OA features with measures of histologic tumor grade. A high total internal OA score was positively, though not significantly, associated with high tumor grade as measured by SBR (Scarff-Bloom-Richardson) total score (A) and its individual components: tubule formation (SBR-T) (B), nuclear atypia (SBR-N) (C), and mitiotic count (SBR-M) (D).

References: Seno Medical Instruments, San Antonio, TX/US

In contrast, the total external OA score, calculated as the sum of the boundary zone and peripheral zone scores, demonstrated an inverse relationship with histopathologic measures of tumor grade (Figure 5), which achieved statistical significance for SBR-TOTAL, SBR-N, and SBR-M, though not for SBR-T.

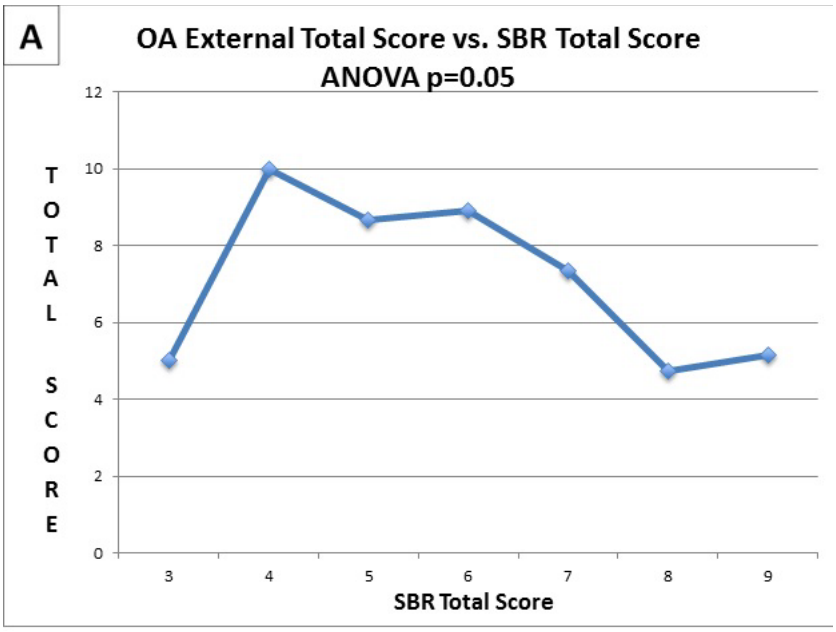
A
OA External Total Score vs. SBR Total Score
ANOVA p=0.05
TOTAL SCORE
0
2
4
6
8
10
12
3
4
5
6
7
8
9
SBR Total Score

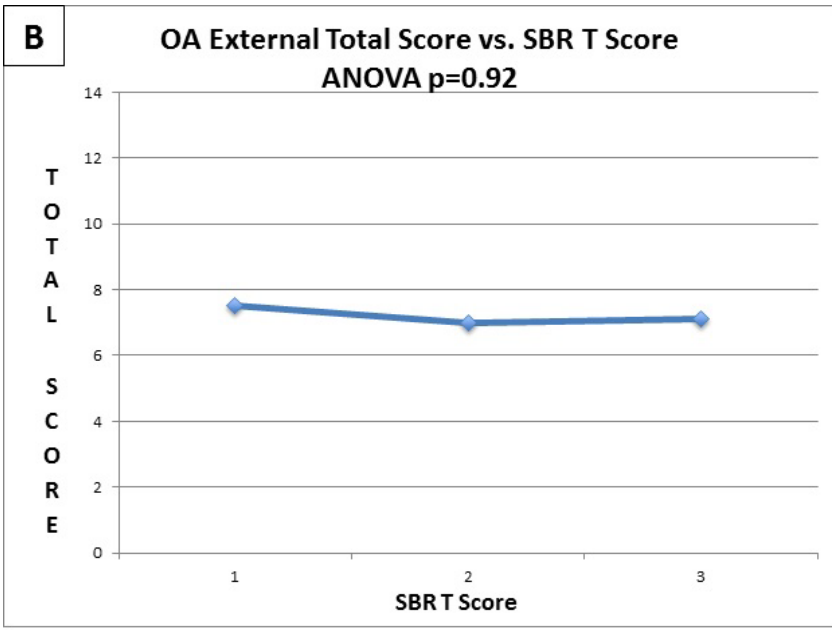
B
OA External Total Score vs. SBR T Score
ANOVA p=0.92
TOTAL SCORE
0
2
4
6
8
10
12
14
1
2
3
SBR T Score

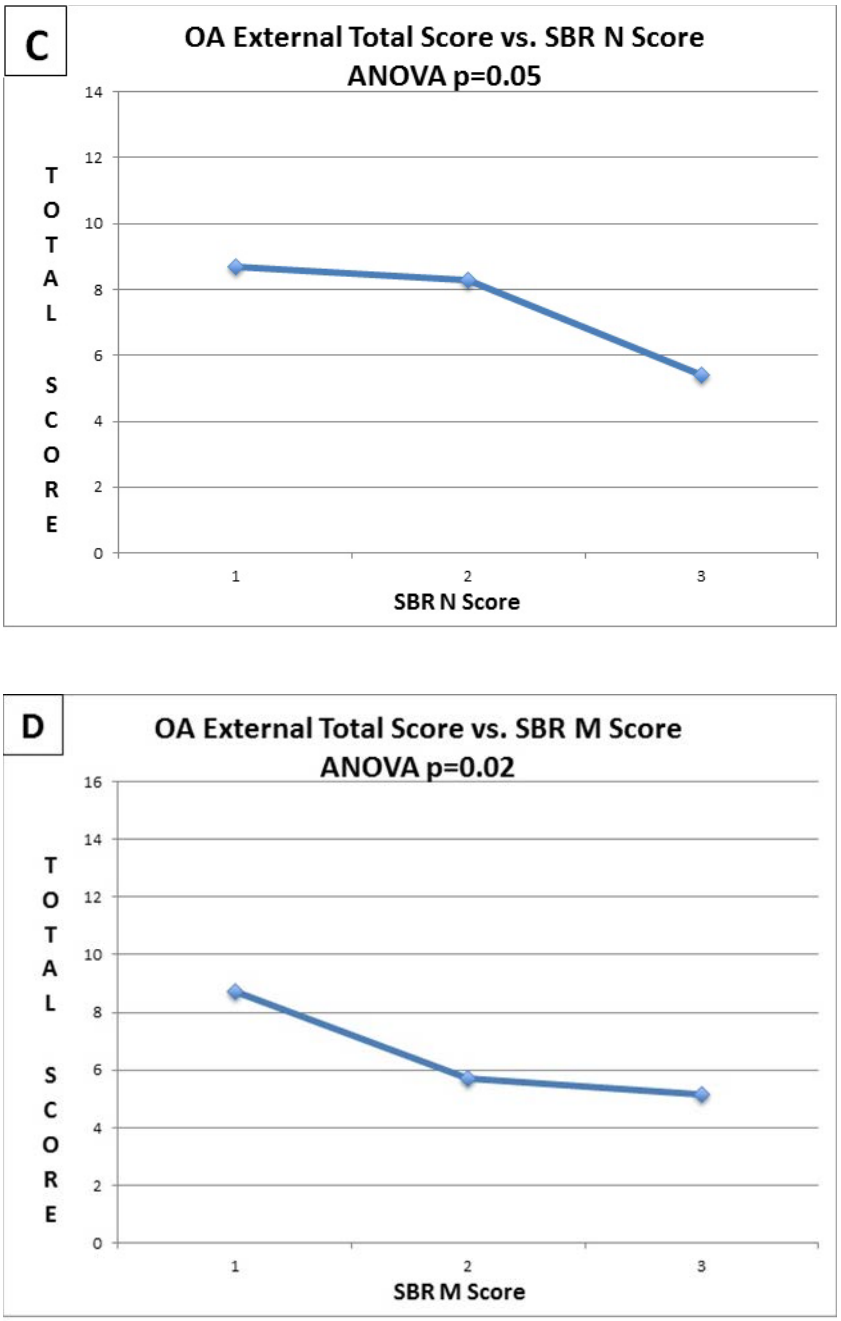

Figure 5. Correlation of external OA features with measures of histologic tumor grade. A high total external OA score was inversely associated with high tumor grade, as measured by SBR (Scarff-Bloom-Richardson) total score (A) and its individual components: tubule formation (SBR-T) (B), nuclear atypia (SBR-N) (C), and mitotic count (SBR-M) (D). Correlations were statistically significant for SBR-TOTAL, SBR-N, and SBR-M.

References: Seno Medical Instruments, San Antonio, TX/US

High-grade tumors appeared to show prominent internal deoxygenated vessels and a relative paucity of external features (Figure 6). Low-grade tumors conversely appeared to show minimal internal vascularity or deoxygenation with prominent boundary zone vascularity and deoxygenation and radiating vessels in the tumor periphery (Figure 7). Intermediate-grade tumors appeared to display a mixture of internal and external OA features (Figure 8).

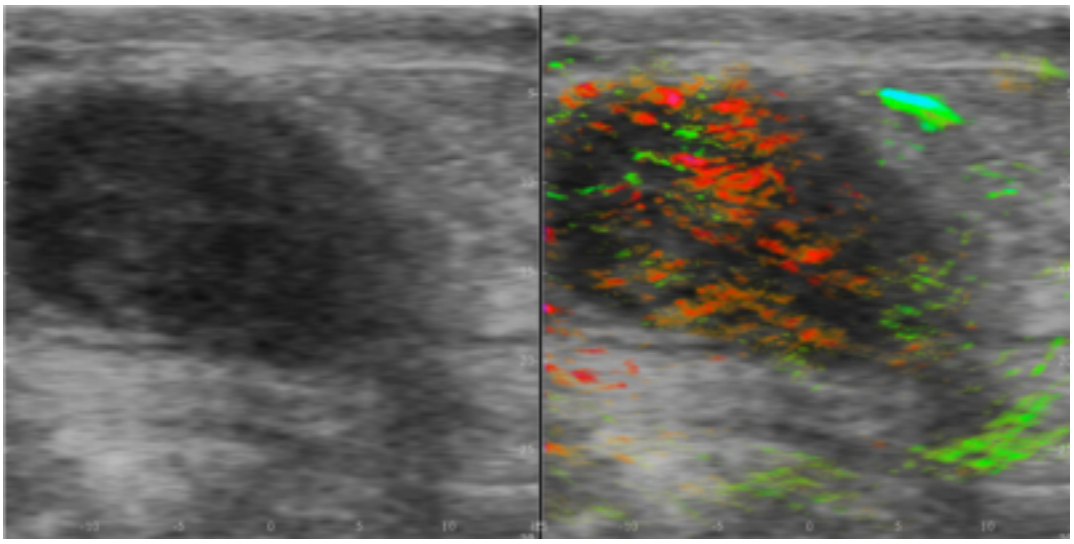

Figure 6. Grade 3 invasive ductal carcinoma showing mainly internal findings. Tumor interior shows increased vascularity with deoxygenated hemoglobin (red); no OA findings are seen in boundary zone and tumor periphery.

References: Seno Medical Instruments, San Antonio, TX/US

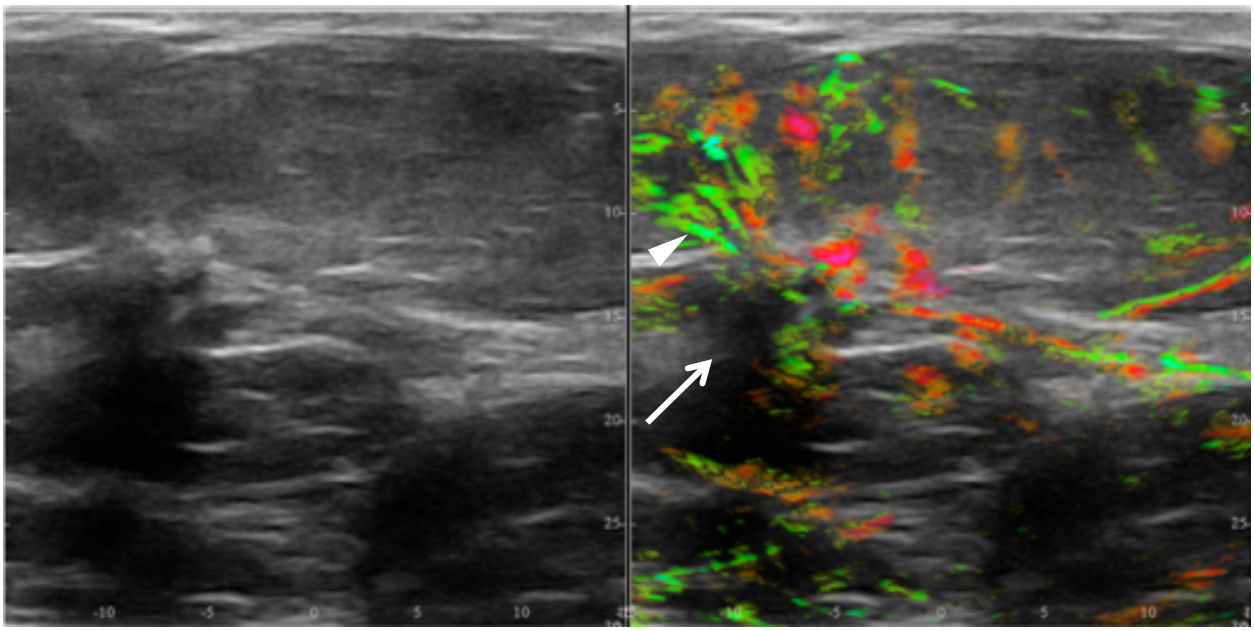

Figure 7. Grade 1 invasive ductal carcinoma showing mainly external findings. Tumor interior shows minimal vascularity with no deoxygenated hemoglobin (arrow); however, tumor periphery demonstrates prominent radiating vessels analogous to architectural distortion on mammography (arrowhead).
References: Seno Medical Instruments, San Antonio, TX/US

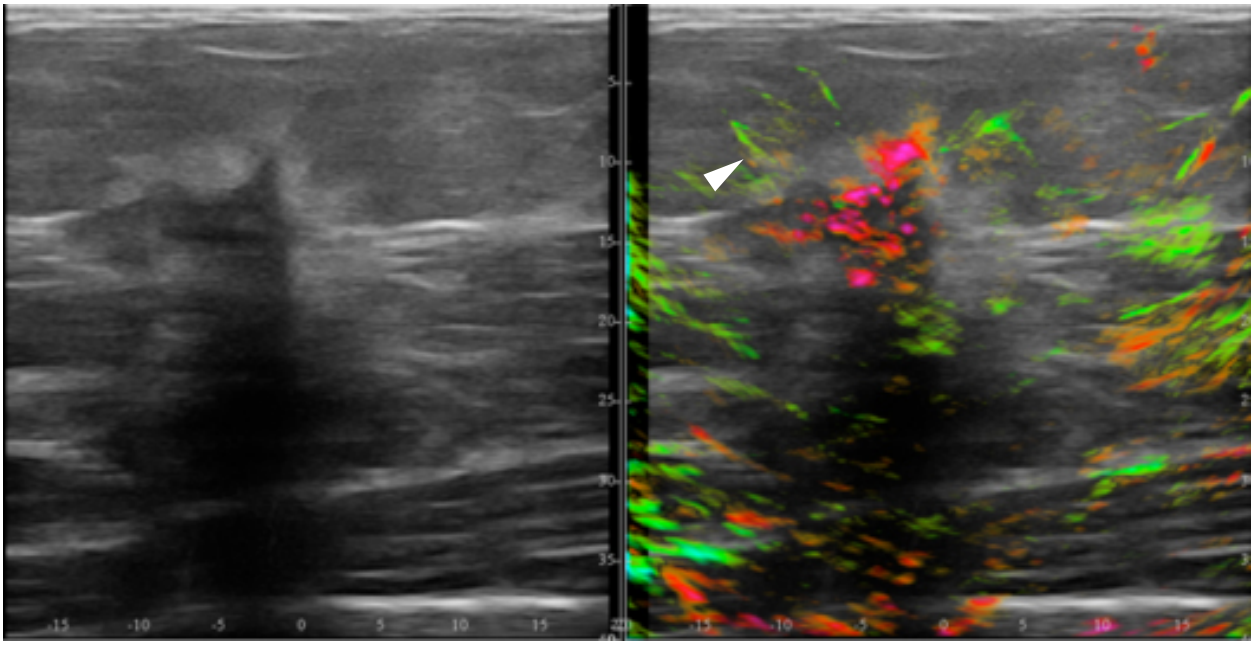

Figure 8. Grade 2 invasive ductal carcinoma showing a mixture of internal and external findings. Tumor interior shows increased vascularity with deoxygenated hemoglobin (pink and red) and tumor periphery shows radiating oxygenated vessels (arrowhead).

References: Seno Medical Instruments, San Antonio, TX/US

Discussion

OA Imaging – Pathology Correlation

Opto-acoustic imaging is a new technology that may be able to demonstrate anatomic tumor morphology and provide functional information about tumor vascularity and deoxygenation without the need for contrast injection or ionizing radiation. OA color maps demonstrate an increased total amount of hemoglobin as well as greater deoxygenation of hemoglobin within and/or surrounding malignant breast tumors. The distribution of these OA features within the tumor interior versus the external boundary zone and periphery correlates with the histologic grade of the malignancies. The histopathologic differences between high and low grade cancers reveal the basis for the OA findings.

Low-grade carcinomas are paucicellular with most of the internal tumor volume comprised of desmoplasia and/or extracellular matrix. The smaller number of tumor cells present are only mildly dedifferentiated. Grade 1 invasive duct carcinomas have relatively few biologically active immune cells. Correspondingly, OA reveals few internal vessels with little or no deoxygenation (Figure 7). Externally, low-grade malignancies demonstrate prominent desmoplasia and peripheral radiating vessels. These histologic features correspond to architectural distortion mammographically and, while difficult to appreciate with conventional ultrasound, are dramatically displayed on OA color maps resulting in a high external OA score. Conversely, high-grade carcinomas are composed of larger numbers of relatively more dedifferentiated tumor cells and also have many biologically active immune cells that rapidly deoxygenate the vascular tumor interior. OA images demonstrate profuse vascularity and deoxygenation within these

tumors, revealing their biologic aggressiveness (Figure 6). Unlike lower grade malignancies, they are characterized by less desmoplasia and few peritumoral radiating vessels resulting in a low external OA score. These aggressive carcinomas more often present as circumscribed masses without associated architectural distortion, overlapping in appearance with benign lesions on anatomic imaging, but tend to have distinctive features on OA imaging due to their high internal vascularity and deoxygenation.

The strong inverse correlation between the total external OA score and biologic aggressiveness may also reflect host immune response. The boundary zone surrounding the growing tumor is frequently a site of an intense and metabolically active immune response. In particular, tumor-associated lymphocytes and macrophages may be present in significant numbers with a consequent positive or negative influence on the biologic aggressiveness of the neoplasm [3]. This peritumoral immune response may contribute to altered depictions of external vascularity and deoxygenation. Thus, a higher external score in prognostically favorable, lower grade malignancies suggests a favorable tumor immune response and merits further study , which would require correlation with numbers and types of leukocytes within the external zones.

OA and Existing Functional Breast Imaging Modalities

As the radiology community strives to continue to improve the accuracy of breast imaging, interest in functional imaging has grown. Elastography has been proposed as a method of improving the accuracy of ultrasound diagnosis on the basis of measuring tumor stiffness. Two forms currently exist, known as strain and shear-wave elastography. In a multinational study, Berg et al. showed that shear-wave elastographic features can be used to selectively downgrade BI-RADS 4a masses and upgrade BI-RADS 3 masses improving specificity from 61.1% to

78.5% [4]. The wide adoption of elastography in clinical practice has been hindered by a number of factors. Inter- and intra-observer variability are relatively high due to dependence on the degree of applied pressure. Elastographic features are less reliable for lesions deeper than 2 cm. Finally, significant false positive and false negative rates are observed due to the presence of soft malignancies and hard benign lesions with reported sensitivities as low as 81.7% for strain elastography and 86% for shear-wave elastography [5-10]. Breast MRI has offered a valuable adjunctive modality based on tumor angiogenesis. While highly sensitive, MRI is limited in its specificity due to the preponderance of vascular benign lesions [11-14]. Furthermore, it requires contrast injection, carries a high cost, and excludes patients with contraindications to exposure to a magnetic field. Scintimammography, another potentially helpful functional modality, is similarly limited by false positive benign lesions, the need for radionuclide injection, and a relatively high total body radiation dose compared to conventional mammography [14, 15]. In addition to the logistic advantages of being relatively low cost without the need for contrast injection or ionizing radiation, OA technology takes functional information to a level beyond imaging the vascularity of tumors, which may be high in both malignant and benign lesions. It further provides a measure of the oxygenation within the vessels of these tumors, which may help to distinguish between benign vascular lesions that remain oxygenated and malignancies which rapidly extract oxygen.

Limitations

Our study has several limitations. It is an early study based on a small number of patients. The analysis of histopathologic features was based primarily on H&E stains. Furthermore, much of the neovascularity and deoxygenation in breast malignancies is within the boundary zone rather than the tumor interior. Conventional pathologic sections do not optimally represent the external

boundary and peripheral zones. Follow-up studies using large section or megacassette histopathologic correlation to better define the causes of external findings, are planned.

Future Directions

These findings are based on a feasibility study. Opto-acoustic imaging is currently undergoing further investigation to validate this data. A prospective multi-institutional pivotal trial in the U.S. (PIONEER) recently completed active enrollment of over 2,000 subjects with follow-up data to be collected by August 2015. Additionally, a post-market clinical follow-up study is soon to be underway in the Netherlands.

The future of OA imaging may potentially include several diverse applications. Aside from improving accuracy in the interpretation of solid breast masses, the technology may play a role in assessing response to neoadjuvant chemotherapy, evaluating axillary lymph nodes, and directing management of high-risk lesions. Furthermore, it may prove useful in organs other than the breast, such as the evaluation of tumors in the prostate or thyroid glands. Further study is needed to elucidate the underlying mechanisms of OA imaging and its potential benefits as a functional imaging platform.

References:

1. Folkman J. Tumor angiogenesis: therapeutic implications. *N. Engl. J. Med*. 1971;285:1182–86
2. Folkman J. Clinical applications of research on angiogenesis. *N. Engl. J. Med.* 1995;333:1757-1763.

3. Mahmoud SM, Paish EC, Powe DG, et al. Tumor-infiltrating CD8+ lymphocytes predict clinical outcome in breast cancer. J Clin Oncol 2011;29(15):1949-1955.
4. Berg WB et al. Shear-Wave Elastography Improves the Specificity of Breast US: The BE1 Multinational Study of 939 Masses. Radiology. 2012;262(2): 435-449
5. Yoon JH et al. Shear-wave elastography in the diagnosis of solid breast masses: what leads to false-negative or false-positive results? Eur Radiol. 2013;23(9):2432-40.
6. Tozaki M et al. Shear wave velocity measurements for differential diagnosis of solid breast masses: a comparison between virtual touch quantification and virtual touch IQ. Ultrasound Med Biol. 2013;39(12):2233-45.
7. Wojcinski S et al. Acoustic radiation force impulse imaging with virtual touch tissue quantification: measurements of normal breast tissue and dependence on the degree of pre-compression. Ultrasound Med Biol. 2013;39(12):2226-32.
8. Shafer FK et al. ShearWave™ Elastography BE1 multinational breast study: additional SWE™features support potential to downgrade BI-RADS®-3 lesions. Ultraschall Med. 2013;34(3):254-9.
9. Chang JM et al. Comparison of shear-wave and strain ultrasound elastography in thedifferentiation of benign and malignant breast lesions. AJR Am J Roentgenol. 2013;201(2):W347-56.
10. Hooley RJ et al. Breast ultrasonography: state of the art. Radiology.2013;268(3):642-59
11. Heywang-Kobrunner SH et al. Magnetic resonance imaging: The evolution of breast imaging. The Breast.2013;22(2):S77-82.
12. Peters NH et al. Meta-analysis of MR imaging in the diagnosis of breast lesions. Radiology.2008; 246(1):116–124

13. Medeiros LR et al. Accuracy of magnetic resonance in suspicious breast lesions: a systematic quantitative review and meta-analysis. Breast Cancer Res Treat.2011;126(2):273–285
14. Bruening W et al. Noninvasive diagnostic tests for breast abnormalities: update of a 2006 review. [Internet] Agency for Healthcare Research and Quality (US), Rockville (MD) (2012 Feb) Report No.: 12-EHC014-EF. AHRQ Comparative Effectiveness Reviews
15. Hendrick RE. Radiation doses and cancer risks from breast imaging studies. Radiology, 257 (1) (2010), pp. 246–253.